Solid–Liquid Equilibria of Mandelic Acid Enantiomers in Two Chiral Solvents: Experimental Determination and Model Correlation

Article *in* Journal of Chemical & Engineering Data · January 2010

DOI: 10.1021/je900353b · Source: OAI

Solid−Liquid Equilibria of Mandelic Acid Enantiomers in Two Chiral Solvents: Experimental Determination and Model Correlation

Samuel Kofi Tulashie,*,† Henning Kaemmerer,‡ Heike Lorenz,† and Andreas Seidel-Morgenstern†,‡

Max Planck Institute for Dynamics of Complex Technical Systems, Sandtorstrasse 1, D-39106 Magdeburg, Germany, and Otto von Guericke University, Institute of Process Engineering, Mailbox 4120, D-39106 Magdeburg, Germany

A study of the ternary solubility phase diagrams of enantiomeric mandelic acid species in the chiral solvents (*S*)-ethyl lactate and (2*R*,3*R*)-diethyl tartrate has been carried out. The solubility measurements were conducted for enantiomeric compositions between the racemic compound and the single enantiomer for temperatures between (273 and 333) K. Experimental results showed no evidence of differences in the solubility of both enantiomers in both chiral solvents. The ideal solubility curves of the mandelic acid species as well as of the racemic compound revealed large deviations from experimental data. The nonrandom two-liquid (NRTL) model was applied to quantify and parameterize the solid−liquid equilibria (SLE) by means of activity coefficients. Hereby, pronounced solute−solute interactions were found, while solvent−solute interactions were interpreted as being nonchiral specific.

Introduction

The majority of the pharmaceutical drugs synthesized are obtained in the form of racemates, that is, as 1:1 mixtures of both enantiomers. Enantiomers play an essential function in biological activity. Normally, biological systems exhibit a well-defined capacity to differentiate between two enantiomers of a compound. Often only one enantiomer exhibits the preferred physiological effect, so there is the need to separate the racemates into their constituent single enantiomers. Hence, the Food and Drug Administration (FDA) demands regulation for enantiopure products.[1] On the basis of the importance of pure single enantiomers and the large chiral market, efficient production of enantiopure substances is very lucrative. Enantioselective crystallization is considered to be an appropriate move toward the separation of enantiomers. Herein, crystallization from chiral solvents[2,3] is an attractive technique in enantioselective crystallization processes, on the basis of the expectation that the solvent can create selective interactions to the chiral molecules and lead to differences in solubilities. These differences might be employed for resolution purposes.

A literature search reveals that there is a lack of systematic experimental work evaluating the application of chiral solvents and quantifying the corresponding solubility data. Moreover, available solubility data of chiral substances in chiral solvents are limited to distinct measurements with the pure enantiomers. For example, Yamamoto and Yamamoto[4] reported pure enantiomer solubilities for a chiral cobalt salt in (2*R*,3*R*)-(+)-diethyl tartrate and described measurable differences between them. Furthermore, Amaya[5] provided a theoretical framework to account for the differences in solubility between D- and L-optical isomers in a chiral solvent, without presenting experimental evidence.

(*S*)- and (*R*)-enantiomers of mandelic acid have been used as resolving reagents in classical resolution for a wide variety of racemates.[6] Furthermore, the pure (*R*)-mandelic acid is used as a precursor for the synthesis of cephalosporin and penicillin.[7] Mandelic acid has bacteriostatic properties, and it is administered for the treatment of urinary tract infections, that is, from either calcium or ammonium salt.[8] The racemic form of mandelic acid is also utilized in the mandelate (ester) form as a relevant pharmaceutical constituent because of its analgesic, antirheumatic, and spasmolytic effects (Mandrophine and Spasmocyclon).[9] The data basis available for mandelic acid is limited to nonchiral solvents. Lorenz et al.[10] determined the ratio of the mandelic acid enantiomers in water at the symmetric eutectic compositions to 0.69 and 0.31. In particular the possibility that the eutectic composition in solution is affected by the presence of the chiral solvent can be of interest for the development of resolution purposes. Linked to the eutectic composition are possible changes to the shape of the solubility isotherms, which are important for process yield estimation. This aspect is not necessarily chiral-specific. Thus, the approach within this paper is not limited to the presence of chiral-specific solute−solvent interactions.

The present work is concerned with a systematic determination of ternary solid−liquid phase equilibria (SLE) of mandelic acid in two chiral solvents, namely, (*S*)-ethyl lactate and (2*R*,3*R*)-diethyl tartrate, in a reasonable temperature range. The ideal solubility of (*S*)-mandelic acid and racemic mandelic acid was calculated and compared to experimental data. The nonrandom two-liquid (NRTL) model was applied to correlate the determined experimental data using activity coefficients. Finally, ternary solubility diagrams were predicted for different solubility isotherms and compared to determined data.

Experimental Section

Materials: Racemic mandelic acid, (*S*)-(+)-mandelic acid (1), and (*R*)-(−)-mandelic acid (2), were supplied from Merck KGaA, Darmstadt, and Sigma-Aldrich Chemical Co. with purities of ≥ 99 %. As solvents, (*S*)-(−)-ethyl lactate (3) and (2*R*,3*R*)-(+)-diethyl tartrate (4) from Fluka/Sigma-Aldrich Chemical Co. with purities of ≥ 99 % were used. For high

* Corresponding author. Phone: (0049) 391 6110 287. Fax: (0049) 391 6110 524. E-mail: tulashie@mpi-magdeburg.mpg.de.
† Max Planck Institute for Dynamics of Complex Technical Systems.
‡ Otto von Guericke University.

10.1021/je900353b CCC: $40.75
Published on Web 10/23/2009

performance liquid chromatography (HPLC) analysis, 2-propanol from Merck KGaA, Darmstadt, with a purity of ≥ 99.5 % was applied.

Apparatus and Procedure: Solubility measurements for mandelic acid were performed in (*S*)-ethyl lactate and (2*R*,3*R*)-diethyl tartrate at temperatures between (0 and 25) °C and (25 and 60) °C, respectively. A classical isothermal method was applied. It involved by preparing a solvent + solute mixture of known composition with solid in excess in a 10 mL glass vessel, which was put into a thermostatted apparatus (RC6 CP Lauda, Germany) and magnetically stirred at a constant temperature (within ± 0.01 K) until equilibrium was attained. Subsequently, the liquid and solid phases were separated and analyzed. For analysis the saturated solution was filtered with a glass filter (pore size of 10 μm), and samples of (1 to 3) mL were withdrawn from the filtrate for double analysis. The concentrations and the enantiomeric excess were determined by means of chiral HPLC after dilution with 2-propanol. An Agilent HP 1100 unit with a Chiralcel OD-H column (Astec, 250 × 4.6 mm/5 μm) was employed. The column temperature was 25 °C, and the flow rate was set to 1.0 mL·min^{-1}. A UV diode array detector was used for peak detection at a wavelength of 254 nm. The eluent fractions by volume were as follows: (a) mandelic acid in (*S*)-ethyl lactate: φ (n-hexane) = 0.84, φ (2-propanol) = 0.16, and φ (trifluoroacetic acid) = 0.001; and (b) mandelic acid in (2*R*,3*R*)-diethyl tartrate: φ (n-hexane) = 0.9, φ (2-propanol) = 0.1, and φ (trifluoroacetic acid) = 0.001.

The solid phases of all samples were studied by X-ray powder diffraction (XRPD), using a PANalytical X'Pert Pro diffractometer (PANalytical GmbH, Germany) with Cu Kα radiation. The samples were measured on Si sample holders and scanned between a diffraction angle of (3 and 40)° with step size of 0.017° and counting time of 50 s per step. These measurements were undertaken to identify the type of species present and also to check for differing solid state forms (solvates and/or polymorphs).

The time needed to attain equilibrium was studied for rac-mandelic acid and (*S*)-mandelic acid in (*S*)-ethyl lactate at 15 °C. Liquid phase samples were collected at defined time intervals from the suspension, and the concentrations were determined by chiral HPLC analysis. Similar experiments were conducted for mandelic acid species in (2*R*,3*R*)-diethyl tartrate. The results illustrated that equilibrium for both solvents was already attained after (3 and 2) h for racemic mandelic acid and (*S*)-mandelic acid, respectively. However, to guarantee thermodynamic equilibration for all measurements conditions, the experimental time was fixed to at least 24 h.

Mole fraction solubility x_i as used for the following equations is defined as:

$$x_i = \frac{n_i}{\sum_{i=1}^{z} n_i} \tag{1}$$

with i being one of the constituents explained above and n_i the molar amount of the latter. The summation covers always the two enantiomers and either (*S*)-(−)-ethyl lactate or (2*R*,3*R*)-(+)-diethyl tartrate. In addition mass fraction solubility w_i according to eq 2 is used in this paper, since this simplifies process design based on graphical representations of, for example, ternary phase diagrams. Herein, m_i represents the mass of the constituent i.

$$w_i = \frac{m_i}{\sum_{i=1}^{z} m_i} \tag{2}$$

To assess the SLE of mandelic acid in (*S*)-ethyl lactate comprehensively, we determined the ternary phase diagram. Thorough solubility measurements were carried out between (0 and 25) °C for the single enantiomers and the eutectic and the racemic compositions. Moreover, to check for asymmetry in the phase diagram, various compositions were measured along the 15 °C isotherm ranging from the racemic compositions to the single enantiomers.

Analogously, solubility measurements were performed for different ratios of mandelic acid enantiomers in (2*R*,3*R*)-diethyl tartrate at temperatures ranging from (25 to 60) °C. The high viscosity of (2*R*,3*R*)-diethyl tartrate at lower temperatures made stirring difficult, but measurements were still feasible.

The reproducibility of the solubility measurements was studied by repeating four experiments under the same conditions. The measurements were conducted with racemic mandelic acid, (*S*)-mandelic acid, and (*R*)-mandelic acid in both (*S*)-ethyl lactate and (2*R*,3*R*)-diethyl tartrate at the lowest and the highest temperatures considered here, that is, at (0 and 25) °C and (25 and 60) °C, respectively. The standard deviations (SD) were calculated by eq 3 with n being the number of experiments and w_k and $\bar{w}$ being the mass fraction solubility and the mean solubility, respectively.

$$\mathrm{SD} = \sqrt{\frac{1}{n-1}\sum_{k=1}^{n}(w_k - \bar{w})^2} \tag{3}$$

The uncertainties are compiled in Table 1. The table contains only the SD for (*S*)-mandelic acid solubilities in the chiral solvents, since the same measurement technique was used for the other mandelic acid species. The SDs for racemic mandelic acid solubilities are in the same range.

Theoretical Section

A first estimation of binary solubility can be derived on the basis of the classical equations by Schröder and van Laar.[3]

In thermodynamic equilibrium the chemical potential of all species in all phases is identical, or more specifically, the fugacity of a dissolved solute equals the fugacity of the undissolved species in the solid state (eq 4).

$$f_i^{l} = f_i^{s} \tag{4}$$

Often, interactions in the solid phase are treated as ideal, and the mutual solubility of both the solid and the liquid phase is neglected. Thus, only the fugacity of the dissolved fraction of the more soluble substance (here: the enantiomers) is considered, and eq 5

Table 1. Error Analysis of Solubility Determination Procedure[a]

t	(*S*)-mandelic acid (1) in (*S*)-ethyl lactate (3)		(*S*)-mandelic acid (1) in (2*R*,3*R*)-diethyl tartrate (4)	
°C	n	SD	n	SD
		100 w		100 w
0	4	0.36		
25	4	0.60	4	0.36
60			4	0.51

[a] SD according to eq 3; number of experiments is n.

$$f_i^l = f_i^{l,0} x_i^{sat} \gamma_i^l \quad (5)$$

can be rearranged into eq 6.

$$\ln\left(\frac{f_i^l}{f_i^{l,0}}\right) = \ln(x_i^{sat}\gamma_i^l) \quad (6)$$

The equation by Schröder and van Laar (eq 7) was applied here in its simplified form (eq 8) without the contribution of the heat capacity terms which tend to compensate mutually.

$$\ln(x_i^{sat}\gamma_i^l) = \frac{\Delta_{fus}H_i}{RT}\left(\frac{T}{T_{m,i}} - 1\right) + \frac{\Delta c_{p,i}}{R}\left(\frac{T_{m,i}}{T} - 1\right) + \frac{\Delta c_{p,i}}{R}\left(-\ln\left(\frac{T_{m,i}}{T}\right)\right) \quad (7)$$

$$\ln(x_i^{sat}\gamma_i^l) = \frac{\Delta_{fus}H_i}{R}\left(\frac{1}{T_{m,i}} - \frac{1}{T}\right) \quad (8)$$

The ideal solubility (x^{sat}_i) of a compound can readily be computed with the knowledge of the calorimetric properties of the solute ($\Delta_{fus}H_i$, $T_{m,i}$) by setting in eq 8 the activity coefficient γ_i^l to unity. The enthalpy of fusion $\Delta_{fus}H_i$ and the melting temperature $T_{m,i}$ of (*S*)-mandelic acid and racemic mandelic acid have been used in this study as determined by Lorenz et al.[10] The increase of solubility with temperature (for a constant enthalpy of fusion) is not related to the type of solvent within this expression, and thus, often additional corrective terms are required to express the real solution behavior. Gibbs excess models have proven to be suitable tools to estimate nonideal behavior of chiral molecules in nonchiral solvents,[11,12] and they are frequently applied to quantify nonideal solvent−solute interactions and to gain better model accuracy. The model parameters of the approaches by Wohl, Margules, Wilson, and also the nonrandom two-liquid model (NRTL) can be found by a fit of model predictions to experimental data, for example, by least-squares routines. Careful parameter identification using experimental data of binary subsystems can allow the prediction of multicomponent systems.[13,14] The models above have in common that they can be extended to include the formation of complexes in the solid phase which is known for the majority of chiral systems.[15] The formation of a racemic compound in the solid phase causes large differences in the solubility, whose magnitudes can be predicted on the basis of the nonideal solubility behavior of the enantiomers. The multicomponent NRTL model eq 9 can be applied to two components ($c = 2$) in the case of a single enantiomer in solution and for three components ($c = 3$) in the case of a racemic mixture of the enantiomers (i,j: constituents).

$$\ln(\gamma_i) = \frac{\sum_{j=1}^{C}\tau_{ji}G_{ji}x_j}{\sum_{j=1}^{c}G_{ji}x_j} + \sum_{j=1}^{c}\frac{x_j G_{ij}}{\sum_{k=1}^{c}x_k G_{kj}}\left(\tau_{ij} - \frac{\sum_{k=1}^{c}x_k\tau_{kj}G_{kj}}{\sum_{k=1}^{c}x_k G_{kj}}\right) \quad (9)$$

The temperature dependency of activity coefficients is incorporated into the model by eqs 10 and 11, introducing two energy parameters, g_{ji} and g_{ij}. The nonrandomness parameter α_{ji} is given by eqs 12 and 13.

$$\tau_{ji} = \frac{g_{ji} - g_{ii}}{RT} \quad (10)$$

$$\tau_{ij} = \frac{g_{ij} - g_{ii}}{RT} \quad (11)$$

$$G_{ji} = \exp(-\alpha_{ji}\tau_{ji}) \quad (12)$$

$$G_{ij} = \exp(-\alpha_{ij}\tau_{ij}) \quad (13)$$

The NRTL model (eq 9) allows the correlation of eq 8 and experimental solubility data. Therefore, a set of three parameters for every binary subsystem is used. In principle there are three binary interactions to consider: (i) solvent and (S)-enantiomer, (ii) solvent and (R)-enantiomer, and (iii) (R)-enantiomer and (S)-enantiomer, leading to nine independent parameters. The species of the racemic compound exists in the solid state only and was not considered for that reason. In principle, systems of enantiomers in nonchiral solvents should allow the substitution of the solute/solvent interactions of one pair by the other and thus the removal of three parameters by assuming $g_{13} = g_{23}$, $g_{31} = g_{32}$, and $\alpha_{13} = \alpha_{23}$. Experimental data must prove whether these assumptions hold for chiral solvents or whether the equalities above are wrong and the six parameters (α_{13}, g_{13}, g_{31}, α_{23}, g_{23}, and g_{32}) need to be determined. In recent literature the heterochiral interactions among the enantiomer pairs are often considered to be negligible.[3,11,16,17] Using this assumption here would allow the removal of a further three parameters (α_{12}, $g_{12,}$, and g_{21}), which simplifies the model significantly. Only the parameters α_{13} (equals α_{31}), g_{13}, and g_{31} remained for that case (eqs 10 to 14). g_{ii} can be chosen freely as a reference state.

The objective function for all parameterizations including the number of experiments N is given by eq 14. A Matlab (MathWorks, U.S.) routine using a Nelder-Mead optimizer with boundary conditions was used to identify suitable NRTL parameters for (*S*)-mandelic acid in the two chiral solvents. Therefore, the difference in the composition-depending solution temperature T^{calc} at saturation and the corresponding T^{exp} in each of the two solvents was minimized.

$$OF = \min\sum_{k=1}^{N}\left(\frac{T_{k,i}^{exp}(x) - T_{k,i}^{calc}(\alpha_{ij}, g_{ij}, g_{ji}, x)}{T_{k,i}^{exp}(x)}\right)^2 \quad (14)$$

Assuming a binary system of two enantiomers, which forms a crystalline compound of 1:1 composition, the eutectic point is found in between a composition consisting of the pure enantiomer only and the racemic compound. The analogue to eq 8 above has been derived by Prigogine and Defay[18] and allows computing the liquidus line with the originating node at the dystectic point and therefore the solubility of the racemic compound. The calorimetric properties of the racemic compound, namely, the enthalpy of fusion and the melting point ($\Delta_{fus}H_{rac}$, $T_{m,rac}$) need to be known.

$$\ln 4x_i x_j = \frac{\Delta_{fus}H_{rac}}{R}\left(\frac{1}{T_{m,rac}} - \frac{1}{T}\right) \quad (15)$$

The analytical derivation for eq 15 is briefly repeated in the Appendix; it reveals resemblance to the equation by Schröder and van Laar (eq 8). The point of intersection of the eqs 8 and 15 gives the eutectic composition of the binary compound forming mixture. It is possible to account for nonidealities in the solubility of the racemic compound by the use of the same activity coefficients as derived for the enantiomers in solution. This holds true as long as heterochiral enantiomer/enantiomer interactions are neglected.

$$\ln[4x_i^{sat}\gamma_i^l x_j^{sat}\gamma_j^l] = \frac{\Delta_{fus}H_{rac}}{R}\left(\frac{1}{T_{m,rac}} - \frac{1}{T}\right) \quad (16)$$

$$\ln[4(x_i^{sat})^2(\gamma_i^l)^2] = \frac{\Delta_{fus}H_{rac}}{R}\left(\frac{1}{T_{m,rac}} - \frac{1}{T}\right) \quad (17)$$

We substitute the fraction of one enantiomer by the fraction of the other, since the racemic compound is present in the liquid phase in form of an equimolar ratio of the two enantiomers. Subsequently, eq 16 can be further simplified and was applied here in form of eq 17.

Results and Discussion

The solubility data measured are summarized in Tables 2 and 3. No additional or new phases were identified other than the racemic compound and the enantiomers from the crystal lattice analysis by XRPD. In Figures 1 and 2 the experimentally determined binary solubilities of both enantiomers, (*S*)-mandelic acid and (*R*)-mandelic acid, and the racemic mandelic acid first in (*S*)-ethyl lactate and second in (2*R*,3*R*)-diethyl tartrate are presented as a function of temperature (symbols). In addition, the ideal solubility of a single enantiomer of mandelic acid and the racemic mandelic acid in the two chiral solvents have been shown (thick lines). The solubility data were in the same range for both solvents at 25 °C, while the racemic mandelic acid was found to be generally better soluble than the single enantiomer. The effect of temperature on solubility is more pronounced in (2*R*,3*R*)-diethyl tartrate for the temperature ranges considered.

While the ideal solubilities of both the racemic mandelic acid and the enantiomer in (*S*)-ethyl lactate and (2*R*,3*R*)-diethyl tartrate were calculated to mass fractions of the enantiomers of 0.04 to 0.1 and 0.05 to 0.16, respectively, the determined values have been much higher (0.17 to 0.25 and 0.14 to 0.27) and thus exhibited a significant deviation from ideal solubility for both chiral solvents. This raised the question of whether the gap is due to speciation of the acid or other pronounced binary interactions with the two solvents. The NRTL model as applied here accounts for the latter, and model parameterization was done with negligible deviations for the (S)-enantiomer. The NRTL model (thin solid lines in Figures 1 and 2) resembles

Table 2. Mass Fraction Solubility (w_i) of (*S*)-Mandelic Acid (1) and (*R*)-Mandelic Acid (2) in (*S*)-Ethyl Lactate (3) at Different Enantiomeric Excesses (ee) [ee = $(w_1 - w_2)/(w_1 + w_2)$] and Temperatures

100 ee	100 $(w_1 + w_2)$	100 w_1	100 w_2	100 w_3
		$t = 0$ °C		
100.00	17.22	17.22	0.00	82.78
37.00	22.20	15.20	7.00	78.80
0.00	21.18	10.59	10.59	78.82
37.36	22.00	6.89	15.11	78.00
100.00	17.20	0.00	17.20	82.80
		$t = 5$ °C		
100.00	18.30	18.30	0.00	81.70
38.32	23.78	16.45	7.33	76.22
0.00	23.07	11.53	11.53	76.94
40.74	24.17	7.16	17.01	75.83
100.00	18.58	0.00	18.58	81.42
		$t = 15$ °C		
100.00	21.50	21.50	0.00	78.50
98.70	21.51	21.37	0.14	78.49
90.34	21.85	20.79	1.06	78.15
72.74	24.99	21.58	3.41	75.01
61.38	24.72	19.95	4.77	75.28
52.68	26.42	20.17	6.25	73.58
42.96	26.78	19.14	7.64	73.22
40.78	28.14	19.81	8.33	71.86
32.16	27.41	18.11	9.30	72.59
22.56	27.72	16.99	10.73	72.28
12.36	25.91	14.56	11.35	74.09
0.00	25.10	12.55	12.55	74.90
2.82	25.17	12.23	12.94	74.83
13.82	25.55	14.54	11.01	74.45
23.96	26.69	16.54	10.15	73.31
35.22	26.50	8.58	17.92	73.50
43.62	27.80	7.84	19.96	72.20
44.20	26.81	7.48	19.33	73.19
55.50	24.95	5.55	19.40	75.05
66.46	24.93	4.18	20.75	75.07
78.08	24.25	2.66	21.59	75.75
87.70	22.21	1.37	20.84	77.79
87.84	22.86	1.39	21.47	77.14
95.00	21.68	0.54	21.14	78.32
100.00	21.50	0.00	21.50	78.50
		$t = 25$ °C		
100.00	25.17	25.17	0.00	74.83
38.00	32.27	22.26	10.01	67.73
0.00	30.61	15.34	15.27	69.39
38.00	32.27	10.01	22.26	67.73
100.00	25.02	0.00	25.02	74.98

Table 3. Mass Fraction Solubility (w_i) of (*S*)-Mandelic Acid (1) and (*R*)-Mandelic Acid (2) in (2*R*,3*R*)-(+)-Diethyl Tartrate (4) at Different Enantiomeric Excesses (ee) [ee = $(w_1 - w_2)/(w_1 + w_2)$] and Temperatures

100 ee	100 $(w_1 + w_2)$	100 w_1	100 w_2	100 w_4
		$t = 25$ °C		
100.00	13.34	13.34	0.00	86.66
66.84	15.08	12.58	2.50	84.92
55.26	17.03	13.22	3.81	82.97
40.36	19.54	13.71	5.83	80.46
1.32	16.84	8.53	8.31	83.16
41.32	20.05	5.88	14.17	79.95
100.00	13.24	0.00	13.24	86.76
		$t = 35$ °C		
100.00	17.03	17.03	0.00	82.97
70.00	19.26	16.37	2.89	80.74
54.48	21.58	16.67	4.91	78.42
38.18	24.93	17.22	7.71	75.07
17.90	23.71	13.98	9.73	76.29
37.02	24.93	7.85	17.08	75.07
0.20	21.36	10.70	10.66	78.64
100.00	17.01	0.00	17.01	82.99
		$t = 45$ °C		
100.00	20.00	20.00	0.00	80.00
76.86	23.25	20.56	2.69	76.75
55.96	26.99	21.05	5.94	73.01
39.94	31.12	21.77	9.35	68.88
23.50	29.15	18.00	11.15	70.85
37.80	31.15	9.69	21.46	68.85
0.20	25.68	12.87	12.81	74.32
100.00	19.11	0.00	19.11	80.89
		$t = 50$ °C		
100.00	22.87	22.87	0.00	77.13
36.72	32.49	22.21	10.28	67.51
37.86	32.30	10.04	22.26	67.70
0.54	29.44	14.80	14.64	70.56
100.00	22.28	0.00	22.28	77.72
		$t = 55$ °C		
100.00	24.15	24.15	0.00	75.85
38.04	36.63	25.28	11.36	63.37
39.02	35.95	10.96	24.99	64.05
0.20	31.66	15.86	15.80	68.34
100.00	24.10	0.00	24.10	75.90
		$t = 60$ °C		
100.00	26.07	26.07	0.00	73.93
36.82	41.98	28.72	13.26	58.02
37.86	40.50	12.58	27.92	59.50
0.54	36.45	18.32	18.13	63.55
100.00	26.31	0.00	26.31	73.69

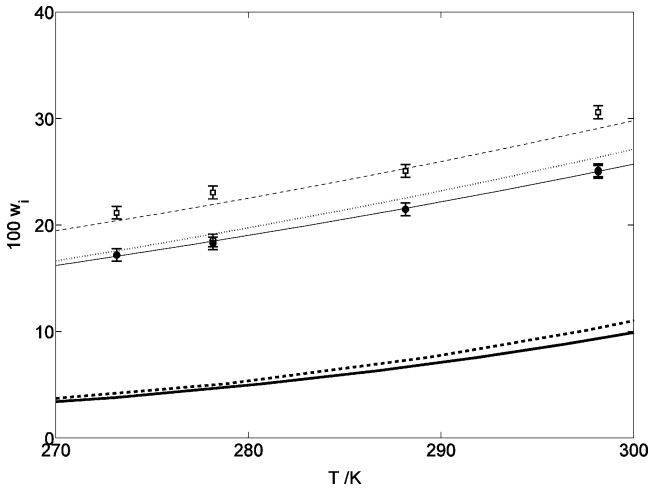

Figure 1. Solubility of ○, (*S*)-mandelic acid (1); ●, (*R*)-mandelic acid (2); and □, racemic mandelic acid ((1) and (2) in equal proportions) in (*S*)-ethyl lactate (3) between (273 and 298) K. Symbols and error bars according to measurements. Lower thick lines: ideal solubility of the enantiomer (solid) and the racemic compound (dashed). Upper thin lines: NRTL model predictions for (*S*)-mandelic acid (solid), racemic mandelic acid w/o heterochiral interactions (dotted), and racemic mandelic acid with heterochiral interactions (dashed).

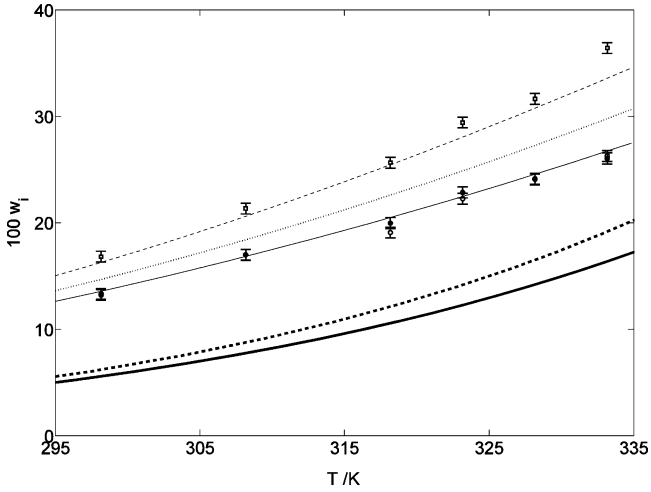

Figure 2. Solubility of ○, (*S*)-mandelic acid (1); ●, (*R*)-mandelic acid (2); and □, racemic mandelic acid ((1) and (2) in equal proportions), in (2*R*,3*R*)-diethyl tartrate (4) between (298 and 333) K. Symbols and error bars according to measurements. Lower thick lines: ideal solubility of the enantiomer (solid) and the racemic compound (dashed). Upper thin lines: NRTL model predictions for (*S*)-mandelic acid (solid), racemic mandelic acid w/o heterochiral interactions (dotted), and racemic mandelic acid with heterochiral interactions (dashed).

the determined values quite closely. Since the solubilities for both enantiomers, (*S*)- and (*R*)-mandelic acid, are the same, the NRTL model was only plotted for the (*S*)-mandelic acid. The binary parameters used and the remaining model deviations are given in Table 4. The prediction of the solubility of the racemic mandelic acid based on the activity coefficients for the enantiomer (dotted line, Figures 1 and 2) was improved significantly in comparison with the large gap between ideal solubility and experimental values. Nevertheless, larger deviations remained. It was assumed that this was due to pronounced heterochiral interactions among the enantiomers, which were not yet incorporated in the model and required a reparameterization of the model by introducing the parameters α_{12}, g_{12}, and g_{21}. The already obtained parameters α_{13}, g_{13}, g_{31}, α_{23}, g_{23}, and g_{32} were set fixed, and eq 14 and the solubility of the racemic compound

Table 4. Binary NRTL Model Parameter for the Two Systems: (*S*)-Mandelic Acid (1) + (*S*)-(−)-Ethyl Lactate (3)/ (2*R*,3*R*)-(+)-Diethyl Tartrate (4)[a]

		solvent	
parameterization		(*S*)-ethyl lactate (3)	(2*R*,3*R*)-diethyl tartrate (4)
α_{1j}		$5.7533 \cdot 10^{-1}$	$4.0104 \cdot 10^{-1}$
g_{1j}		-2.9342 kJ·mol^{-1}	$2.5269 \cdot 10^{4}$ kJ·mol^{-1}
g_{j1}		$3.1028 \cdot 10^{4}$ kJ·mol^{-1}	$-3.2356 \cdot 10^{3}$ kJ·mol^{-1}
model deviation	enantiomer	$7.8386 \cdot 10^{-6}$ K	$3.9479 \cdot 10^{-5}$ K
	racemic compound	$3.8 \cdot 10^{-3}$ K	$3.3 \cdot 10^{-3}$ K
α_{12}		$1.9408 \cdot 10^{-3}$	$9.79748 \cdot 10^{-1}$
g_{12}		$-1.0042 \cdot 10^{5}$ kJ·mol^{-1}	$2.16631 \cdot 10^{5}$ kJ·mol^{-1}
g_{21}		$1.06910 \cdot 10^{5}$ kJ·mol^{-1}	$1.41879 \cdot 10^{5}$ kJ·mol^{-1}
model deviation	enantiomer	$7.8386 \cdot 10^{-6}$ K	$3.9479 \cdot 10^{-5}$ K
	racemic compound	$7.4707 \cdot 10^{-5}$ K	$3.3155 \cdot 10^{-5}$ K

[a] Deviation from experimental data is calculated according to eq 14 with and without additional parameters (α_{12}, g_{12}, and g_{21}) to account for heterochiral interactions.

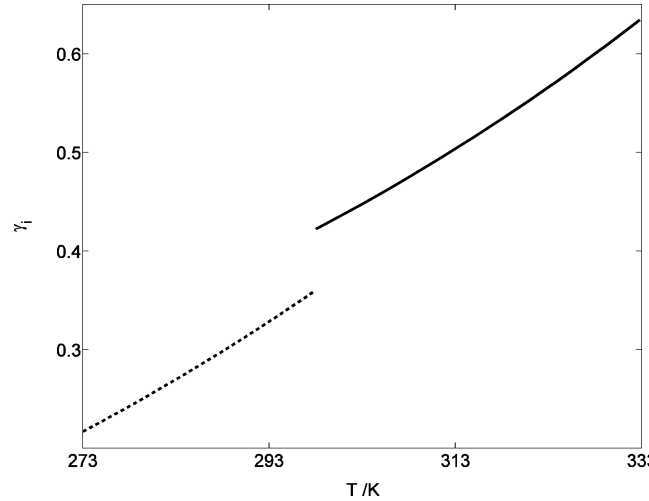

Figure 3. Activity coefficients of mandelic acid enantiomers (homochiral) in (*S*)-ethyl lactate (dashed line) and (2*R*,3*R*)-diethyl tartrate (solid line) at saturation in the considered temperature range.

were used to estimate suitable parameters to express the heterochiral solute−solute interactions. The obtained additional parameters and the remaining errors for both systems are given in Table 4.

The rather large deviations from ideality in both chiral solvents is exemplified in Figure 3 by means of plotting the theoretical activity coefficients of the (*S*)-mandelic acid as a function of temperature. While the values in (2*R*,3*R*)-diethyl tartrate were already far from unity, the deviation from ideality in (*S*)-ethyl lactate is even more pronounced. The small activity coefficients account for the large solubility difference between ideal and experimentally observed solubility. In addition, the order of nonideality in the two solvents is visible.

A more comprehensive compilation of the activity coefficients according to the NRTL model also for under-/ and supersaturated solutions is given in Figures 4 and 5. The activity coefficients relevant for the determined solubility isotherms can be found on the thick lines and correspond to the values in Figure 3.

Figures 6 and 7 compare the predicted ternary solubility phase diagrams and measurements of the mandelic acid enantiomers in (*S*)-ethyl lactate and (2*R*,3*R*)-diethyl tartrate,

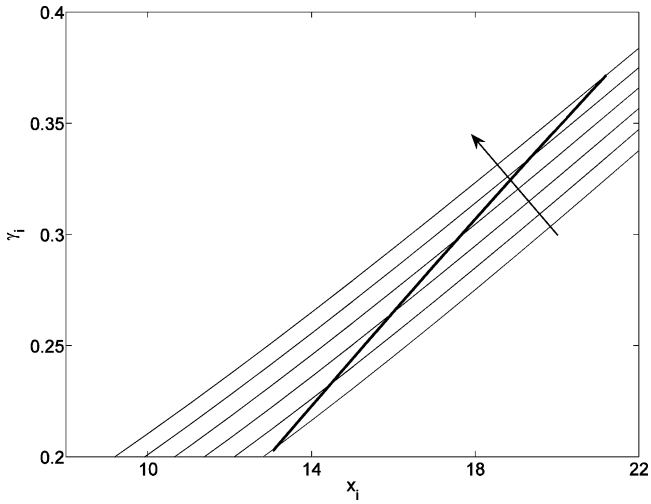

Figure 4. Temperature (arrow points towards higher temperatures, T = (270.15, 276.15, 282.15, 288.15, 294.15, and 300.15) K) and composition dependency of activity coefficients of mandelic acid enantiomers (homochiral) in (*S*)-ethyl lactate according to the NRTL model for the given temperatures and solution compositions. Activity coefficients of the saturated solution as used in Figures 1 and 3 are shown additionally (thick line).

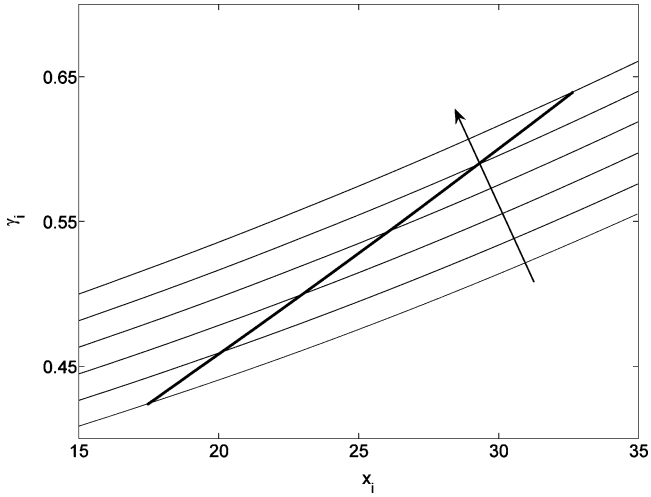

Figure 5. Temperature (arrow points towards higher temperatures, T = (298.15, 305.15, 312.15, 319.15, 326.15, and 333.15) K) and composition dependency of activity coefficients of mandelic acid enantiomers (homochiral) in (2*R*,3*R*)-diethyl tartrate according to the NRTL model for the given temperatures and solution compositions. Activity coefficients of the saturated solution as used in Figures 2 and 3 are shown additionally (thick line).

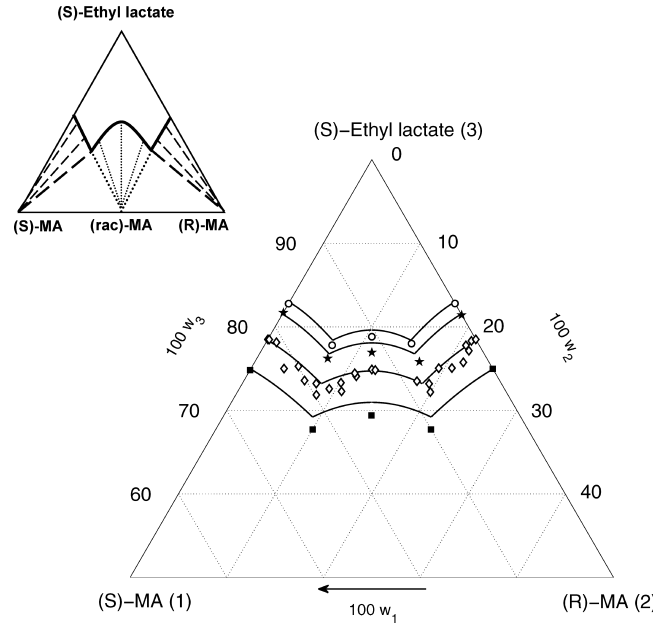

Figure 6. Predicted ternary phase diagram of the mandelic acid enantiomers in (*S*)-ethyl lactate (3): according to the NRTL model and measurement data for four solubility isotherms (○, 273.15 K; ★, 278.15 K; ◊, 288.15 K; and ■, 298.15 K). Schematic overview (figure, upper left) with proposed tie lines linking the corresponding solid phases.

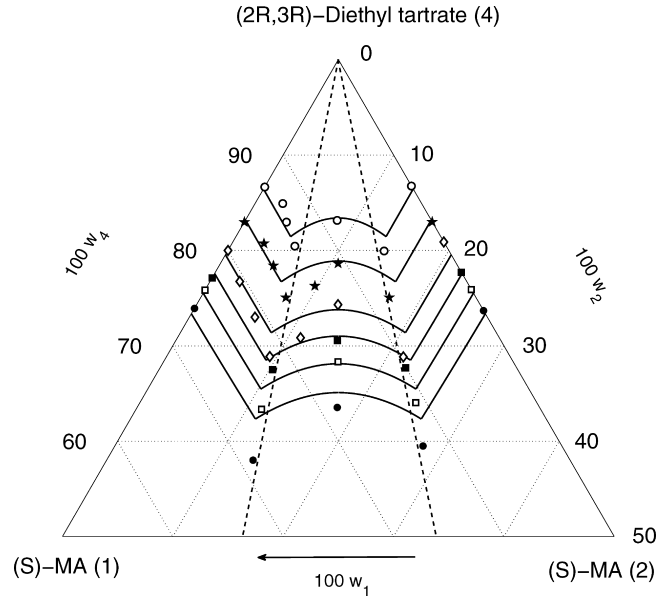

Figure 7. Predicted ternary phase diagram (upper section) of the mandelic acid enantiomers in (2*R*,3*R*)-diethyl tartrate (4) according to the NRTL model and measurement data for five solubility isotherms (○, 298.15 K; ★, 328.15 K; ◊, 318.15 K; ■, 323.15 K; □, 328.15 K; and ●, 333.15 K). The dashed lines highlight eutectic compositions.

respectively. The liquid phase is in equilibrium with the corresponding solid phase of the crystalline enantiomer (Figure 6, left upper corner, dashed tie lines) for ratios of the enantiomers within (0 to 31) % and (69 to 100) %, while ratios of (31 to 69) % of the enantiomers in the liquid phase are in equilibrium with the crystalline racemic compound (Figure 6, left upper corner, dotted tie lines). The solubility isotherms confirm the compound-forming character of the mandelic acid system. The diagrams show symmetrical mirror images with respect to the racemic axis rather than asymmetrical ones which are generally possible in the case of chiral solvents. The symmetry verification was supported by detailed measurement of the solubility isotherm at 15 °C. The predicted solubility isotherms are in good agreement with the measured solubility points in (*S*)-ethyl lactate in particular for lower temperatures. The determined solubility points in (2*R*,3*R*)-diethyl tartrate are worse when represented by the NRTL model prediction; the agreement is again better for lower temperatures. The solubilities in the outer two-phase region of the phase diagram are better captured than those for the inner two-phase region. The worst agreement is found for the solubilities at the eutectic compositions, while the eutectic compositions are fairly good when derived by the model. The ratio of the enantiomers at the symmetric eutectic compositions remained unchanged with temperature at 0.69 and 0.31 (dashed lines, Figure 7) in both solvents as it was also reported in earlier results for nonchiral solvents.[10] The same general shape of the solubility isotherm was observed

in both figures. Considerations with regard to crystallization-based separation of mandelic acid enantiomers taking into account solution thermodynamics and kinetics by applying chiral solvents are described in refs 19 and 20.

Conclusions

The SLE of the compound-forming system mandelic acid in two chiral solvents, (*S*)-ethyl lactate and (2*R*,3*R*)-diethyl tartrate, were studied. Detailed solubility data in the ternary systems have been presented and compared to model predictions. No asymmetry in the ternary solubility phase diagram was found with respect to the thermodynamic properties, which implies that there was no distinct chiral recognition in the liquid state between the chiral solute and the chiral solvent molecules. Consequently, the deviation from ideal solubility is not enantioselective and could be treated as nonchiral. Thus, it was possible to substitute the model parameters for the (*S*)-mandelic acid−solvent interactions by (*R*)-mandelic acid−solvent interaction parameters. Solubility data of one enantiomer were correlated with the NRTL model to derive the solubility of the racemic compound. It was shown that heterochiral interactions between the mandelic acid enantiomers cannot be neglected, since a larger gap remained between the predicted solubility of the racemic compound and the experimental values. Therefore, the NRTL model was extended by three parameters to account for these (symmetric) heterochiral interactions, and model predictions were improved.

Appendix

The analytical solution to equation 16 by Prigogine and Defay is briefly repeated in the following. It is helpful to introduce the total differential of the Gibbs free energy to relate the chemical potential to affinity (eqs I and II).

$$\mathrm{d}G = \left(\frac{\partial G}{\partial T}\right)_{p,n}\mathrm{d}T + \left(\frac{\partial G}{\partial p}\right)_{T,n}\mathrm{d}p + \sum_{\mathrm{i}}\mu_{\mathrm{i}}\mathrm{d}n_{\mathrm{i}} \qquad \text{(I)}$$

A partial derivation of the Gibbs free energy with respect to a reaction progress variable ξ at constant pressure and temperature links eq I to the affinity A of (eq II). Prigogine and Defay used a similar expression, while we refer here to eq II according to IUPAC.[18]

$$-\left(\frac{\partial G}{\partial \xi}\right)_{T,p} = A \qquad \text{(II)}$$

$$A = \mu^{\mathrm{s}}_{\mathrm{rac}} - \nu_{\mathrm{i}}\mu^{\mathrm{l}}_{\mathrm{i}} - \nu_{j}\mu^{\mathrm{l}}_{\mathrm{j}} \qquad \text{(III)}$$

For assumed isothermal/isobaric conditions, equilibrium between the formation of the racemic compound in the solid phase and the corresponding two dissolved enantiomers can be derived as shown in eq III. The indices i,j of eq III represent the chemical potential of the two counter enantiomers in the liquid phase, while the racemic compound (solid phase) is represented by $\mu^{\mathrm{s}}_{\mathrm{rac}}$. The stoichiometric coefficients $\nu_{\mathrm{i/j}}$ for each enantiomer can be set to unity, since the racemic compound is considered to consist of equimolar amounts of the two enantiomers. The affinity or, analogously, the derivative of the Gibbs free energy becomes zero in thermodynamic equilibrium, and here the chemical potential of the solid racemic compound will equal the sum of the chemical potentials of the enantiomers in the liquid phase.

Equation IV was derived by Prigogine and Defay[18] from the total differential of the affinity A over temperature. For a negligible pressure change and a differential change in the affinity of dA the equation V can be followed.

$$\mathrm{d}\left(\frac{A}{T}\right) = \frac{H}{T^2}\mathrm{d}T - \frac{V}{T}\mathrm{d}p + \frac{1}{T}\left(\frac{\partial A}{\partial x}\right)_{T,p}\mathrm{d}x \qquad \text{(IV)}$$

$$\mathrm{d}(A) = \frac{A+H}{T}\mathrm{d}T + \left(\frac{\partial A}{\partial x^{\mathrm{l}}_{\mathrm{j}}}\right)_{T,p}\mathrm{d}x^{\mathrm{l}}_{\mathrm{j}} \qquad \text{(V)}$$

Partial derivation of eq III with respect to the composition $\partial A/\partial x$ and the Gibbs−Duhem equation for a binary system yields eq VI. In thermodynamic equilibrium the affinity as well as the differential of the affinity becomes zero, and eq VII follows.

$$\frac{\partial A}{\partial x^{\mathrm{l}}_{\mathrm{j}}} = \nu_{\mathrm{i}}\cdot\left(\frac{x^{\mathrm{l}}_{\mathrm{j}}}{x^{\mathrm{l}}_{\mathrm{i}}} - \frac{\nu_{\mathrm{j}}}{\nu_{\mathrm{i}}}\right)\cdot\frac{\partial \mu^{\mathrm{l}}_{\mathrm{j}}}{\partial x^{\mathrm{l}}_{\mathrm{j}}} \qquad \text{(VI)}$$

$$\frac{\partial T}{\partial x^{\mathrm{l}}_{\mathrm{j}}} = -\frac{\nu_{\mathrm{i}}T\cdot\left(\frac{x^{\mathrm{l}}_{\mathrm{j}}}{x^{\mathrm{l}}_{\mathrm{i}}} - \frac{\nu_{\mathrm{j}}}{\nu_{\mathrm{i}}}\right)\cdot\frac{\partial \mu^{\mathrm{l}}_{\mathrm{j}}}{\partial x^{\mathrm{l}}_{\mathrm{j}}}}{H} \qquad \text{(VII)}$$

Equation X can be derived using the equations above in conjunction with the definition of the chemical potential of an ideal system (eq VIII) and its derivation with respect to composition (eq IX).

$$\mu = \mu^{\circ}(p,T) + RT\ln x \qquad \text{(VIII)}$$

$$\left(\frac{\partial \mu^{\mathrm{l}}_{\mathrm{j}}}{\partial x^{\mathrm{l}}_{\mathrm{j}}}\right)_{T,p} = \frac{RT}{x^{\mathrm{l}}_{\mathrm{j}}} \qquad \text{(IX)}$$

$$\left(\frac{\nu_{\mathrm{j}}}{x_{\mathrm{j}}} - \frac{\nu_{\mathrm{i}}}{x_{\mathrm{i}}}\right)\partial x_{\mathrm{j}} = \frac{H}{RT^2}\partial T \qquad \text{(X)}$$

A racemic composition of $x_{\mathrm{i/j}} = 0.5$ is usually chosen as the lower integration boundary, and the melting temperature and the heat of fusion of the racemic compound ($\Delta_{\mathrm{fus}}H_{\mathrm{rac}}$, $T_{\mathrm{m,\ rac}}$) are applied. This leads to eq XI, which can be transferred through simple algebra to the known expression of eq XII.

$$-\ln\frac{x_{\mathrm{i}}x_{\mathrm{j}}}{0.25} = \frac{\Delta_{\mathrm{fus}}H_{\mathrm{rac}}}{R}\left(\frac{1}{T} - \frac{1}{T_{\mathrm{m,rac}}}\right) \qquad \text{(XI)}$$

$$\ln 4x_{\mathrm{i}}x_{\mathrm{j}} = \frac{\Delta_{\mathrm{fus}}H_{\mathrm{rac}}}{R}\left(\frac{1}{T_{\mathrm{m,rac}}} - \frac{1}{T}\right) \qquad \text{(XII)}$$

Acknowledgment

The authors thank V. Subbarayudu-Sistla, C. Malwade, A. Hayoun, J. Kaufmann, and L. Borchert for the help in the experimental work.

Literature Cited

(1) Maier, N. M.; Franco, P.; Lindner, W. Separation of enantiomers: needs, challenges, Perspectives. *J. Chromatogr., A* **2001**, *906*, 3–33.
(2) Reichardt, C. *Solvents and Solvent Effects in Organic Chemistry*, 3rd ed.; VCH: Weinheim, 2003.
(3) Jacques, J.; Collet, A.; Wilen, S. H. *Enantiomers, racemates and resolutions*; Krieger Publishing Company: Malabar, FL, 1994.
(4) Yamamoto, M.; Yamamoto, Y. Stereospecific solute-solvent interaction between Δ-(+)$_{\mathrm{D}}$ or Δ-(−)$_{\mathrm{D}}$-Co (en)$_3$ $^{3+}$ and L-(+)$_{\mathrm{D}}$-diethyltartrate appeared in solubility and viscosity. *Inorg. Nucl. Chem. Lett.* **1975**, *11*, 833–836.
(5) Amaya, K. Statistical Thermodynamics of Solutions of Optically Active Substances II. Solubility of d- and l-Isomers in Optically Active Solvents. *Bull. Chem. Soc. Jpn.* **1961**, *34*, 1803–1806.
(6) Acs, M.; Novotny-Bregger, E.; Simon, K.; Argay, G. Structural Aspects of Optical Resolutions. Optical Resolution of (R, S)-

Mandelic Acid. DSC and X-ray Studies of the Diastereoisomeric Salts. *J. Chem. Soc., Perkins Trans.* **1992**, *2*, 2011–2017.
(7) Yamazaki, Y.; Kajiwara, S. Enzymatic synthesis of D-mandelic acid. *Bio Ind.* **1988**, *5*, 261–268.
(8) Reynolds, J. E. F., Ed. *Martindale: The Extra Pharmacopoeia*, 30th ed.; The Pharmaceutical Press: London, 1993.
(9) Elvers, B., Ed. *Ullmann's Encyclopedia of Industrial Chemistry*; VCH: Weinheim, 1989.
(10) Lorenz, H.; Sapoundjiev, D.; Seidel-Morgenstern, A. Enantiomeric Mandelic Acid System-Melting Point Phase Diagram and Solubility in Water. *J. Chem. Eng. Data* **2002**, *47*, 1280–1284.
(11) Worlitschek, J.; Bosco, M.; Huber, M.; Gramlich, V.; Mazzotti, M. Solid-Liquid Equilibrium of Tröger's Base Enantiomers in Ethanol: Experiments and Modelling. *Helv. Chim. Acta* **2004**, *87*, 279–291.
(12) Kaemmerer, H.; Polenske, D.; Lorenz, H.; Seidel-Morgenstern, A. In *Selection and application of chiral resolution strategies for compound forming systems on the basis of solubility isotherms*. Proc. 15th BIWIC, Magdeburg, Germany, 2008; Lorenz, H., Kaemmerer, H., Eds.; Shaker: Aachen, Germany; pp 42−49.
(13) Renon, H.; Prausnitz, J. M. Local compositions in thermodynamic excess functions for liquid mixtures. *AIChE J.* **1968**, *14*, 135–144.
(14) Sandler, S. I. In *Chemical, Biochemical, and Engineering Thermodynamics*, 4th ed.; John Wiley & Sons, Inc.: New York, 2006.
(15) Kaemmerer, H.; Lorenz, H.; Seidel-Morgenstern, A. In *Theoretical and experimental determination of solid-liquid equilibria of chiral compound forming systems in solution*. Proc. 17th ISIC, Maastricht, The Netherlands, Sept 14−17, 2008; Jansens, J. P., Ulrich, J., Eds.; pp 479−486.
(16) Wang, Y. Eutectic Composition of a Chiral Mixture Containing a Racemic Compound. *Org. Process Res. Dev.* **2005**, (9), 670–676.
(17) Wang, Y.; Chen, A. M. Purification of Partially Resolved Enantiomeric Mixtures with the Guidance of Ternary Phase Diagram. *Org. Process Res. Dev.* **2008**, *12*, 282–290.
(18) Prigogine, I.; Defay, R. *Chemical Thermodynamics*; Longmann: London, U.K., 1973.
(19) Tulashie, S. K.; Lorenz, H.; Hilfert, L.; Edelmann, F. T.; Seidel-Morgenstern, A. Potential of Chiral Solvents for Enantioselective Crystallization. 1. Evaluation of Thermodynamic Effects. *Cryst. Growth Des.* **2008**, *8*, 3408–3414.
(20) Tulashie, S. K.; Lorenz, H.; Seidel-Morgenstern, A. Potential of Chiral Solvents for Enantioselective Crystallization. 1. Evaluation of Kinetic Effects. *Cryst. Growth Des.* **2009**, *9* (5), 2387–2392.

Received for review April 14, 2009. Accepted October 9, 2009.

JE900353B